

## **SILICA NANOPARTICLES PRODUCED BY THERMAL ARC PLASMA. MODELLING**

E. Balabanova\*

Institute of Electronics, Bulgarian Academy of Sciences, Tzarigradsko Chaussee 72,  
Sofia 1784, Bulgaria

The presented work summarises our results concerning the modelling of silica vapour-to-silica nanoparticles generation in both forms - non-aggregated and aggregated, realised in a thermal arc plasma set up. It is shown that some operating parameters, such as initial temperature of the vapour and the vapour supersaturation, play important role in the mechanism of particle formation and growth, and in the structure of the produced particles, respectively.

(Received July 10, 2003; accepted July 31, 2003)

*Keywords:* Silica nanoparticles, Thermal arc plasma modelling

### **1. Introduction**

In the recent years the powders containing silica nanoparticles have been used in a lot of applications as fillers (reinforcing agents for producing "green tires"), lubricants (tixotropic additions for liquids), additions ("free-flow" agents for toners), silica based catalysts (molecular sieves), etc. [1-3]. The various applications need powders with different structure, for example: for reinforcing agents powders containing aggregates are suitable, for catalytic activity, on the contrary, unaggregated powders are preferable. The structure depends on the method of powder production. The flame methods that are conventionally used for silica nanopowders production usually produce large nanoparticle structures- aggregates [4-6]. In [7, 8] we had shown that in a thermal arc plasma set up for manufacturing of silica sand to silica nanopowders, there is an opportunity for generation of silica nanoparticles in two forms - non-aggregated and aggregated. The study of the unique conditions (thermal, hydrodynamic, kinetic etc.) in the plasma set up leads to a better understanding of the processes for the nanoparticle synthesis. By modelling these processes, it is possible to get information about the relation between the operating parameters and the particle structure.

The presented work summarises our results concerning the modelling of silica vapour-to-silica nanoparticles generation in non-aggregated and aggregated form.

### **2. Modelling the processes carried out in thermal arc plasma set up**

#### **2.1. Vaporisation of silica sand**

Argon plasma jets or direct arc are used in our stationary plasma furnace for the sand vaporisation. The electric power of the arc is in the range 18-30 kW. The sand vaporisation is combined with SiO<sub>2</sub> destruction to SiO and oxygen. Because of that it is suitable to use reductors,

---

\* Corresponding author: emilia@ie.bas.bg

which bound the oxygen and shift the  $\text{SiO}_2$  destruction process to the right side, i.e. increasing vaporisation.

Experiments were made without and with use of reductor carbon during the sand vaporisation. The experimental characteristics (specific surface area, mean surface diameter and median mean diameter) of two samples of silica powders, obtained in two regimes were discussed [8]. The samples were produced at the following initial mole ratios:  $\text{SiO}_2:\text{Ar} = 1:1.4$  and  $\text{SiO}_2:\text{Ar}:\text{C} = 1:14:1$ . It was shown that the sample, produced with use of carbon contained aggregate structures.

To understand the conditions for the sand vaporisation in both experiments, in the present work thermodynamic equilibrium calculations are made for the systems  $\text{SiO}_2\text{-Ar}$  and  $\text{SiO}_2\text{-Ar-C}$ . The calculations concern temperature range 1500-3500 K and pressure 1 atmosphere. The standard program is used for calculation of chemical equilibrium contents.

## 2.2. Silica vapour- to-silica nanoparticle conversion

Silica vapour-to-silica nanoparticle conversion is carried out in plasma flow reactor (see the diagram given in Fig. 1).

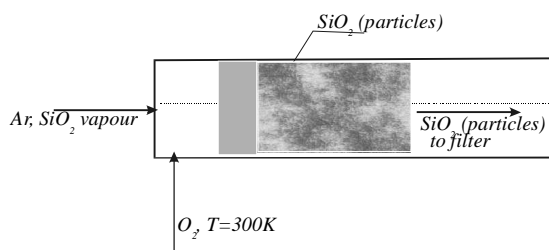


Fig. 1. Diagram of the plasma flow reactor for silica nanoparticle production.

In the reactor the hot flow (silica vapour and plasma gas) coming from the plasma furnace (vaporiser) is mixed with a cooling flow ( $\text{O}_2$ ). The cooling flow, with temperature of 300 K, enters the reactor transversely to the hot flow. The cooling gas is taken in a big excess to the silica vapour. The initial ratios are  $\text{SiO}_2:\text{Ar}:\text{O}_2 = 1:1.4:10$  and  $\text{SiO}_2:\text{Ar}:\text{C}:\text{O}_2 = 1:14:1:25$ , respectively. During the mixing temperature variation of the flow is observed, chemical reactions between the components of the hot flow and the cooling gas as well as, nanoparticle generation are carried out.

The model of the processes in our aerosol flow reactor is developed previously [9]. It includes the presentation of: the fluid dynamics; the thermal- and the mass- balances of the flow; the chemical processes for nanoparticle precursor synthesis and the nanoparticle growth by free-molecular coagulation.

Below are shown the equations presenting the fluid dynamics, the energy- and the mass balances

$$\frac{d(\rho u)}{dx} = \sum_{i=1}^n m_i g_i^{\text{mix}}(x); \quad (1)$$

$$\rho = \sum_{i=1}^n m_i c_i \quad (2)$$

$$\frac{dc_i}{dx} = \frac{g_i}{u} - \frac{c_i}{u} \frac{du}{dx} + \frac{g_i^{\text{mix}}(x)}{u}; \quad i=1, \dots, n \quad (3)$$

$$\frac{dp}{dx} + \frac{d(\rho u^2)}{dx} = 0; \quad (4)$$

$$p = RT \sum_{i=1}^n c_i \quad (5)$$

$$\frac{d}{dx} \left[ u \left\{ \frac{\rho u^2}{2} + \sum_{i=1}^n H_i(T) c_i \right\} \right] = \sum_{i=1}^n [g_i^{mix}(x) H_i(T^{mix})] \quad (6)$$

where:  $x$  is the axial co-ordinate;  $u$  is the velocity;  $\rho$  is the density;  $T$  is the temperature of the gas mixture;  $T^{mix}$  is the temperature of the mixing gas;  $p$  is the pressure;  $R$  is the gas constant;  $n$  is the number of components;  $m_i$ ,  $c_i$ ,  $H_i$ , are the molecular mass, the volume concentration and the enthalpy of the  $i$ -th component, respectively;  $g_i$ ,  $g_i^{mix}$  are the source terms presenting the variation of the  $i$ -th component quantity in unit volume in unit time due to chemical reactions and mixing, respectively.

The term  $g_i^{mix}$ , presenting the cooling gas ( $O_2$ ) variation, is approximated by the linear function

$$g_{O_2}^{mix}(x) = \frac{g_2 - g_1}{x_2 - x_1} x \quad (7)$$

where  $x$  is axial co-ordinate;  $g_2 - g_1 = 1$  is the full quantity of the mixing gas;  $x_2 - x_1$  is equal to the mixing length. It is known that the mixing length depends on the reactor diameter and on the diameter and the place of the cooling gas orifice. This length for the mixing of transverse flows (as it is in our case) is considered to be  $3d$  [9].

The model considers the chemical reactions carried out between silica vapour ( $SiO$ ) and cooling gas ( $O_2$ ). In the cases when carbon is used for the sand vaporisation, reactions between  $CO$  and  $O_2$  are included too.

The list of reactions is:



The reactions (8) and (9) lead to production of the precursor of silica nanoparticles,  $SiO_2$  gas molecule. The conversion rate of  $SiO$  to  $SiO_2$  ( $\kappa$ , %) is an important parameter presenting the  $SiO$  oxidation processes.

$$\kappa = \frac{[SiO]}{[SiO] + [SiO_2]} 100, \quad \% \quad (13)$$

where  $[SiO]$  and  $[SiO_2]$  are the mole fractions of the corresponding species.

The further conversion of the precursors to nanoparticles is the homogeneous nucleation and free-molecular coagulation. Such conversion can be realised when the silica vapour reaches high supersaturation. The supersaturation is determined by the saturation ratio ( $S$ ) which is the ratio between the  $\text{SiO}_2$  mole fraction in the gas mixture (vapour partial pressure) and the saturated vapour pressure at the corresponding temperature.

In our model the particle growth via free-molecular coagulation is presented by a discrete-sectional method, described in [10]. In this method the particles are included in discrete groups (sections), depending on their masses -  $m$ ,  $2^2m$ ,  $2^n m$ , where  $m$  is the mass of the precursor. The set of equations used in the method is:

$$\frac{dz_n}{dt} = \sum_{l < n-1} 2^{l-n} C_{l,n} z_n z_l + \frac{3}{4} C_{n-1,n-2} z_{n-1} z_{n-2} + \frac{1}{2} C_{n-1,n-1} z_{n-1}^2 - \sum_{l=n-1}^M C_{n,l} z_n z_l - \lambda z_n \quad (14)$$

$$\frac{dz_0}{dt} = -z_0 \sum_{l=1}^M C_{o,l} z_l - \lambda z_0 \quad (15)$$

$$C_{n,l} = \left(2^{n/3} + 2^{l/3}\right)^2 \left(\frac{1+2^{n-l}}{2^n}\right)^{1/2} F(m, \rho, T) \quad (16)$$

$$F(m, \rho, T) = 2^{1/6} 3^{2/3} m^{1/6} \pi^{-1/6} \rho^{-4/6} (kT)^{1/2} \quad (17)$$

Here  $z_n$ ,  $z_l$  are the number concentrations of particles in groups  $n$  and  $l$  ( $\text{cm}^{-3}$ );  $z_0$  is the precursor concentration.  $M$  is the number of groups;  $C_{nl}$  is the coagulation coefficient for the particle groups ( $\text{cm}^3/\text{s}$ );  $\rho$  is the mass density of the particles, (for silica particles it is taken to be  $2.2 \text{ g/cm}^3$ ),  $k$  is Boltzmann's constant,  $T$  is absolute temperature. The term  $\lambda z_n$  presents the variation of the particle concentration with the variation of the volume during the cooling of the gas mixture in the reactor.

After solving the set of equations 14-17, one gets the particle size distribution function (PSDF).

### 3. Results and discussion

To determine the silica vapourisation temperature in both considered systems ( $\text{SiO}_2$ -Ar and  $\text{SiO}_2$ -Ar-C), thermodynamic calculations are made. In them the initial mole ratios of the components correspond to that of the experiments, namely  $\text{SiO}_2:\text{Ar}=1:1.4$  and  $\text{SiO}_2:\text{Ar}:\text{C}=1:14:1$ . The equilibrium contents, obtained after thermodynamic calculations, are presented in the Figs. 2 and 3.

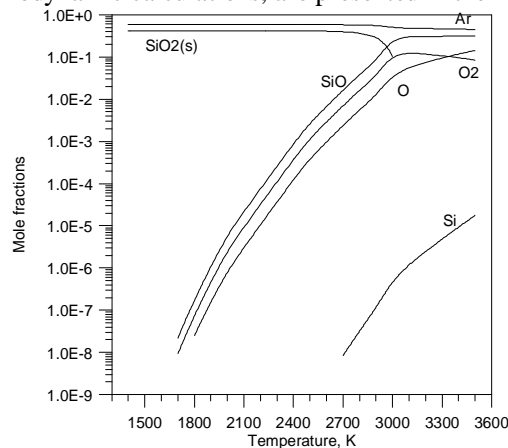


Fig. 2. Equilibrium content of the species in the vaporiser calculated for the initial mole ratio  $\text{SiO}_2 : \text{Ar} = 1:1.4$ .

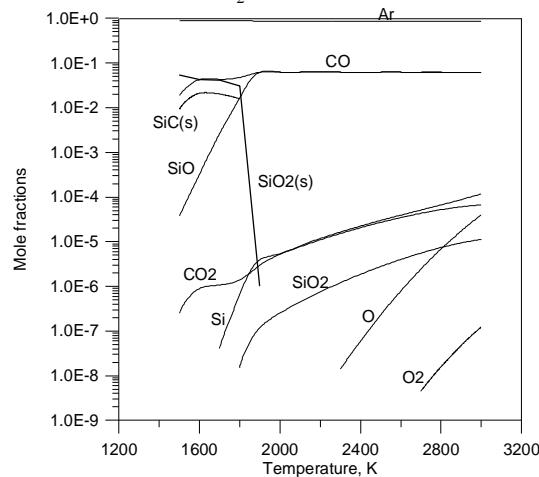


Fig. 3. Equilibrium content of the species in the vaporiser, calculated for the initial mole ratio  $\text{SiO}_2 : \text{Ar} : \text{C} = 1:14:1$ .

The results show that in the system without carbon, homogeneous equilibrium (without  $\text{SiO}_2$ -solid fraction in the system) is reached at the temperature of 3000 K. In the system  $\text{SiO}_2:\text{Ar}:\text{C}=1:14:1$  homogeneous equilibrium is reached at 2000 K. The observed lower value of the  $\text{SiO}_2$  vaporisation temperature is explained by the chemical reactions between silica vapour and carbon (bonding of the oxygen) and also with the larger ratio  $\text{SiO}_2 : \text{Ar}$  used in this case. The influence of different initial ratios  $\text{SiO}_2 : \text{Ar}:\text{C}$  on the vaporisation was discussed previously [11]. It was established that large ratios  $\text{SiO}_2 : \text{Ar}$  and also the use of C decrease the vaporisation temperature.

As it was mentioned above, in the flow reactor the hot gas mixture (silica vapour and plasma gas) and cooling gas ( $\text{O}_2$ ) are mixed and oxidation of  $\text{SiO}$  to  $\text{SiO}_2$  is carried out. The rate of  $\text{SiO}$  to  $\text{SiO}_2$  conversion plays important role in the complex processes realised in the reactor. In Figs 4 and 5 the variation of the conversion rate ( $\kappa$ ) and the variation of the  $\text{O}_2$ -amount, entering the reactor ( $g_{\text{O}_2}^{\text{mix}}$ ) are shown for the cases without and with use of carbon, respectively. It can be seen that in both cases the  $\text{SiO}$  oxidation is finished very soon after the start of the  $\text{O}_2$  mixing. The time of the complete  $\text{SiO}$  oxidation (time when  $\kappa=0$ ) is called "oxidation time". The time of the complete  $\text{O}_2$  mixing is called "mixing time". The comparison of these times for both cases show that they are shorter when one uses carbon.

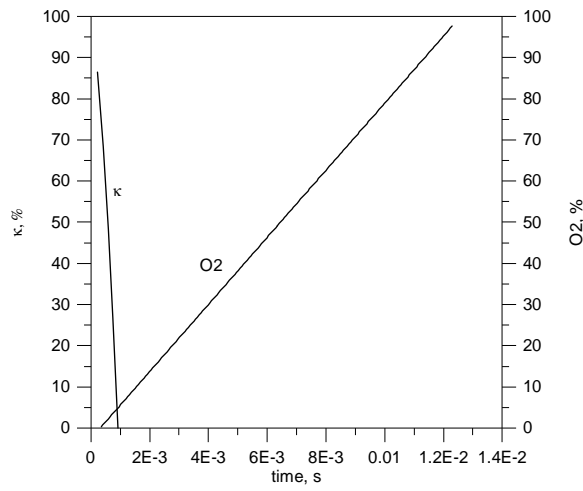


Fig. 4. Evolution of the SiO conversion rate ( $\kappa$ ) and of the  $O_2$  amount, introduced in the flow reactor ( $g^{mix}_{O_2}$ ), calculated for the mole ratio  $SiO_2 : Ar : O_2 = 1:1.4:10$ .

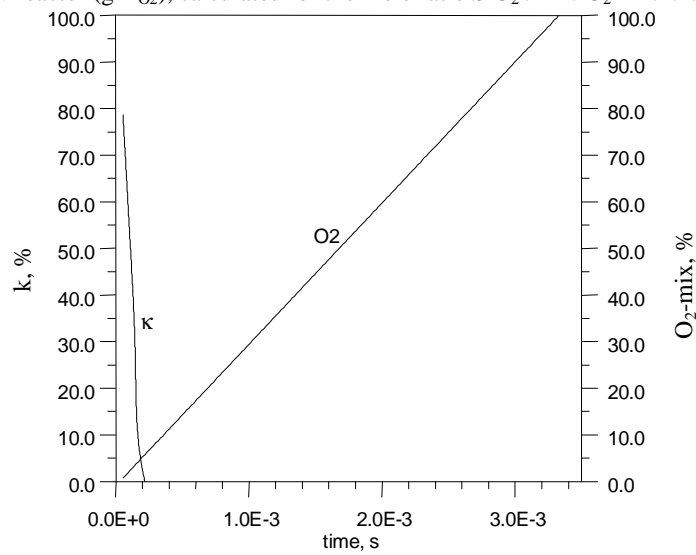


Fig. 5 Evolution of the SiO conversion rate ( $\kappa$ ) and of the  $O_2$  amount, introduced in the flow reactor ( $g^{mix}_{O_2}$ ), calculated for the mole ratio  $SiO_2 : Ar : C : O_2 = 1:14:1:25$ .

The flow temperature and the vapour supersaturation are other important parameters. Their variations are shown in Fig. 6.

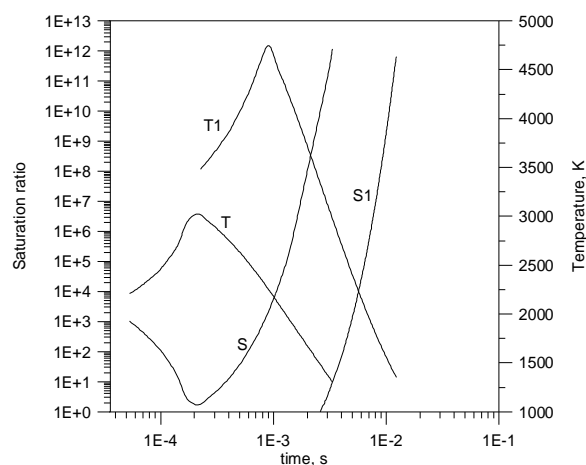


Fig. 6 Evolution of the temperature and the saturation ratio during the  $O_2$  mixing in the flow reactor, in the cases of:  $SiO_2$ : Ar: C:  $O_2 = 1:14:1:25$  (T, S) and  $SiO_2$ : Ar:  $O_2 = 1:1.4:10$  (T1, S1).

In both cases an initial increasing of the temperature can be seen. This is explained by the exothermic effect of the oxidation reactions. After the complete SiO oxidation (at  $t=9.084 \times 10^{-4}$  s and  $t=2.176 \times 10^{-4}$  s, respectively) the temperature drops with a constant rate until the end of the cooling gas mixing (i.e. to  $t_m = 1.229 \times 10^{-2}$  s and  $t_m=3.34 \times 10^{-3}$  s, respectively).

In the case of pure silica vapour, the initial temperature increases from 3000 K to over 4700 K during the complete SiO oxidation. The saturated vapour pressure is very high in this temperature range and the  $SiO_2$  partial pressure can not reach it, so there is no opportunity for cluster formation during the oxidation. The supersaturation is reached after the complete oxidation, long after the start of the mixing. Three different values of supersaturation (7.6, 75 and 195) have been chosen as initial values for the homogeneous nucleation and the free-molecular coagulation onset. Using eqs. 14-17, the corresponding particle size distribution functions (PSDFs) are calculated (see Fig. 7). The choice of the supersaturation is arbitrary, since we do not have experimental proof of the supersaturation at which the process starts. In Fig. 7 the experimental PSDF is also shown. As it is seen the best agreement between the experimental and the calculated PSDFs is observed at the highest supersaturation.

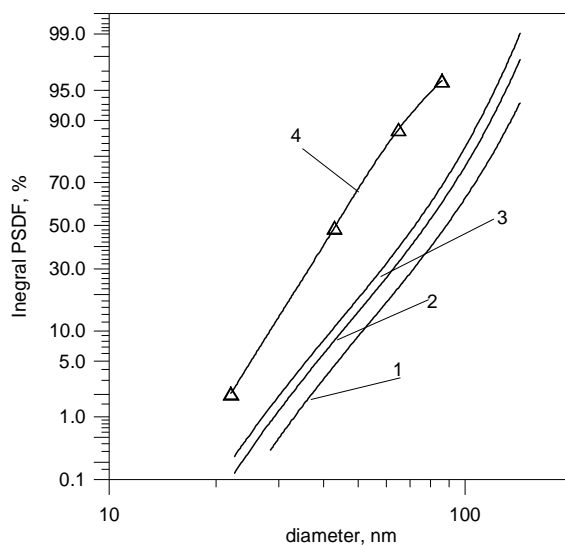


Fig. 7. PSDFs calculated at the supersaturation: 7.6 (1), 75 (2), 195 (3); experimental PSDF (4).

In the case when carbon is used during the vaporisation, the initial temperature of the gas mixture, entering in the reactor is 2000 K. At this temperature, the SiO<sub>2</sub> saturated vapour pressure is very low, and it can be easily reached and overreached. Even the small SiO<sub>2</sub> mole fraction, obtained at the beginning of SiO oxidation is quite enough for reaching a large supersaturation. After that during the oxidation, since the temperature increases very fast and the corresponding saturation vapour pressure becomes very high, the saturation ratio decreases. When the oxidation is completed and the temperature starts to decrease, the saturation ratio increases constantly. This type of variation of the saturation ratio suggests a more complicated mechanism of nanoparticle growth, compared to those of pure silica vapour. We could not apply free-molecular coagulation model (eqs.14-17) directly because the vapour condensation at the very beginning of the mixing is carried out simultaneously with chemical oxidation reactions. A new model is needed in which the influence of the chemical source of precursors on coagulation should be estimated. The coalescence (fluid fusion) of the particles must be considered, too. It is known that near to temperature 2000 K the SiO<sub>2</sub> particles can not completely fuse because of the high viscosity of SiO<sub>2</sub> at this temperature, so the production of aggregate structures becomes possible. We have some experimental results, proving the content of nanoparticle aggregates in a sample which is produced with use of carbon [ 8].

#### 4. Conclusion

The conditions for production of silica nanoparticles in thermal arc plasma set up are discussed for two experimental cases. It is shown that some operating parameters such as initial vapour temperature and vapour supersaturation are important for the mechanism of particle formation and growth, and, respectively, for the structure of the produced particles.

#### References

- [1] A. Blume, B. Freund, in "Silica 98", Mulhouse, France, 1-4 Sept., 261, 1998.
- [2] H. Barthel, M. Dreyer, T. Gottschalk-Gaudig in "Silica 2001", Mulhouse, France, 3-6 Sept. 2001, report number 68.
- [3] G. Schulz, R. Fricke, G Lischke, B. Parlitz, ISPC-11, Loughborough, England, 1993, editor J. Harry, p.112-117.
- [4] D. W. Schaefer, A. Hurd, *Aerosol Science and Technology*, **12**, 876 (1990).
- [5] W. Koch, S. Fridlander *J. Colloid and Interface Science*, **140**, 419 (1990)3
- [6] M. Choi, J.Lee, H.W. Kim, *Journal of Nanoparticle Research*, **1**, 169 (1999).
- [7] E. Balabanova, D. Oliver in "Silica 2001", Mulhouse, France, 3-6 Sept. 2001, report number 142.
- [8] E. G. Balabanova, D. H. Oliver, in: "Nanoscience & Nanotechnology '02", editors E. Balabanova, I. Dragieva, Heron press, Sofia, 29, 2002
- [9] E. Balabanova, *Vacuum* **69**, 207 (2003).
- [10] E.G. Balabanova, A. A. Levitsky, D. H. Oliver: *Czech. J. Phys.* **44**, 139 (1994).
- [11] E. Balabanova, in "Silica 98" Mulhouse, France, 1-4 Sept., 67, 1998.